

Biomechanical analysis of the effects of medial meniscectomy on degenerative osteoarthritis

Ji Yong Bae · Kyung Soon Park · Jong Keun Seon ·
Dai Soon Kwak · Insu Jeon · Eun Kyoo Song

Received: 18 May 2011 / Accepted: 10 October 2011 / Published online: 26 October 2011
© International Federation for Medical and Biological Engineering 2011

Abstract To investigate the effects of meniscectomy on degenerative osteoarthritis, a three-dimensional (3D) finite element (FE) model of the human lower limb is constructed from a combination of magnetic resonance (MR) images and computed tomographic (CT) images that can provide anatomically suitable boundary conditions for a knee joint. Four cases, i.e., the intact meniscus, and the partial, sub-total, and total meniscectomy of the medial meniscus are modeled and simulated. We consider that the cartilage-to-cartilage contact area and the peak contact pressure in the meniscus may be significant parameters in evaluating degenerative osteoarthritis. Partial meniscectomy can be regarded as a better treatment than sub-total/total meniscectomy, and a high possibility of degenerative osteoarthritis is anticipated after total meniscectomy. Moreover, medial meniscectomy has the potential to bring about degenerative osteoarthritis in both the medial compartment and the lateral compartment of a knee joint.

Keywords Meniscectomy · Contact area · Contact pressure · Degenerative osteoarthritis · Finite element analysis

1 Introduction

Meniscectomy is an orthopedic operation to excise some part of the meniscus. This procedure has been widely performed to treat various meniscal injuries caused by an external force or a degenerative tear [12, 15, 23]. However, clinical follow-up results after partial meniscectomies have shown that the incidence of significant degenerative osteoarthritis and the rate of reoperation increase after meniscectomy; therefore, patient satisfaction decreases [12, 23]. In addition, long-term follow-up studies after total meniscectomy have demonstrated a high incidence of degenerative change and poor functional results for knee joints compared to the results from partial meniscectomy [11, 18].

Experimental studies have been carried to understand the effects of meniscectomy on knee joints in terms of contact area and pressure. According to Fukubayashi and Kurosawa [9], degenerated knees have a larger contact area than intact knees due to wear at the articular cartilage and osteophyte formation in the peripheral region of the tibial plateaus. Burke et al. [8] reported that the removal of more of the central part of the meniscus increases the peak stress in the tibial plateau. Other researchers have shown that contact pressure increases by 3–9 times compared to intact knee joints after partial and total meniscectomy [3, 25].

Computational studies of meniscectomy procedures have been performed using numerical models of knee joints. Using discrete element analysis, Segal et al. [26] showed that contact stress is a risk factor for the progress of

J. Y. Bae · I. Jeon (✉)
School of Mechanical Systems Engineering, Chonnam
National University, 300 Yongbong-dong, Buk-gu,
Gwangju 500-757, Republic of Korea
e-mail: i_jeon@chonnam.ac.kr

K. S. Park · J. K. Seon · E. K. Song
The Center for Joint Disease, Hwasun Hospital, Chonnam
National University, 160 Ilsimri, Hwasun-Eup, Hwasun-Gun,
Jeonnam 519-809, Republic of Korea

D. S. Kwak
Department of Anatomy, Catholic Institute for Applied
Anatomy, College of Medicine, The Catholic University
of Korea, 505 Banpo-dong, Seocho-gu, Seoul 137-040,
Republic of Korea

incident symptomatic osteoarthritis. Bendjaballah et al. [5] used a three-dimensional (3D) finite element (FE) model to examine the distribution of loading in the medial and lateral plateaus of tibio-femoral joints and load transmission through menisci in full extension. Peña et al. [19] developed a 3D FE model of the femorotibial joints using MR images to evaluate the effects of meniscal tears and various meniscectomies in full extension, and estimated the contact area and pressure distributions between menisci and articular cartilage. Wilson et al. [28] suggested an axisymmetric model of the knee joint using linear elastic materials.

These experimental and computational studies give a rough understanding of the biomechanical behavior and mechanisms between menisci and articular cartilage; this is because the models considered only an axial loading state and not the moment of the knee joint that is applied to the lower limb bony structure. To the best of our knowledge, only Yang et al. [29] has considered the physiological loading conditions obtained from inverse dynamic analysis and a muscle force reduction model obtained from subject-specific data. They evaluated the combined effect of the frontal plane tibiofemoral angle after partial and total meniscectomy on the stress and strain in the knee cartilage. However, they used a partial model around the tibiofemoral joints. Therefore, their study has a limitation regarding the simulation of actual knee joints. There are no meniscectomy studies reported in the literature that consider anatomically suitable boundary conditions including the lower limb structure, ligaments, and muscle forces.

To investigate the effects of meniscectomy on degenerative osteoarthritis considering anatomically suitable boundary conditions, we developed a 3D FE model of the human lower limb based on a combination of MR images and CT images. In particular, four cases (the intact meniscus, and the partial, sub-total, and total meniscectomized medial meniscus) were modeled. FE analysis (FEA) using the lower limb model was performed for each case to estimate the contact area and contact pressure representing the normal part of the contact stress in the femoral and tibial articular cartilage and the menisci. These two contact parameters are known to be closely related to degenerative osteoarthritis of the knee joint after meniscectomy [9, 26].

2 Methods

2.1 Data acquisition

T1 magnetic resonance (MR) images and computed tomographic (CT) images were obtained from the healthy left knee joint of a 26-year-old male. The MR scan was performed using a 3T-MR scanner (Tim Trio, Siemens,

Germany) around the knee joint under full extension. The CT scan was performed using a 64-channel volume CT scanner (Light Speed, General Electric Company, USA) from the sacrum to the femur under full extension. MR images were obtained at intervals of 0.7 mm in the sagittal plane. The acquisition parameters were a field of view of 140×140 mm, an optimal pixel size of 0.275 mm, and a resolution of 512×512 pixels. CT images were obtained at intervals of 2.5 mm in the axial plane. The optimal pixel size was approximately 0.49 mm with a resolution of 512×512 pixels.

2.2 Reconstruction and combination of the lower limb

The MR images were used to reconstruct distal 7 cm of the femur and proximal 6.5 cm of the tibia, and entire parts of the fibula and patella, articular cartilage, meniscus, ligaments, and tendons. The CT images were used to reconstruct lower limb bony structures such as the sacrum, coxal bone, femur, and tibia. All the reconstruction processes were accomplished using MIMICS software (v10.1, Materialise, Belgium). To match the positional coordinates of each model, anatomical reference points were defined as the central point of the diaphysis of the femur, the midpoint of the transepicondylar axis, and the intercondylar notch in the reconstructed CT and MR models. The process of combining the reconstructed CT and MR models with this positional alignment for each model was achieved by using commercial software Rapidform[®] (v2006, INUS Technology, Inc., Korea).

2.3 Finite element modeling and material properties

A FE model of the lower limb was constructed with the six aforementioned bony structures and their articular cartilages, menisci, ligaments, tendons, and muscles (Fig. 1a, b) using the commercial software PATRAN (v2008, MSC Software Corporation, USA). The total number of elements and nodes used for the lower limb model was 338,588 and 501,883, respectively. Because, it is well known that the bone strain was much smaller than the strain in soft tissues such as the articular cartilage and menisci [6, 10], the entire bony structure was considered as a rigid body. For all the parts except the ligaments, tendons, and muscles, quadratic tetrahedral solid elements with ten nodes were used and homogeneous, isotropic, and linear elastic material properties were applied as shown in Table 1 [2, 4, 6, 10, 16, 17, 26, 27, 30]. In fact, the menisci and cartilage need to be assumed as anisotropic and viscoelastic materials. However, considering the time independent and simple compressive load applied to the knee joint (i.e., five-sixths of the body weight), the menisci and cartilage were assumed to be homogeneous, isotropic, and linear elastic materials.

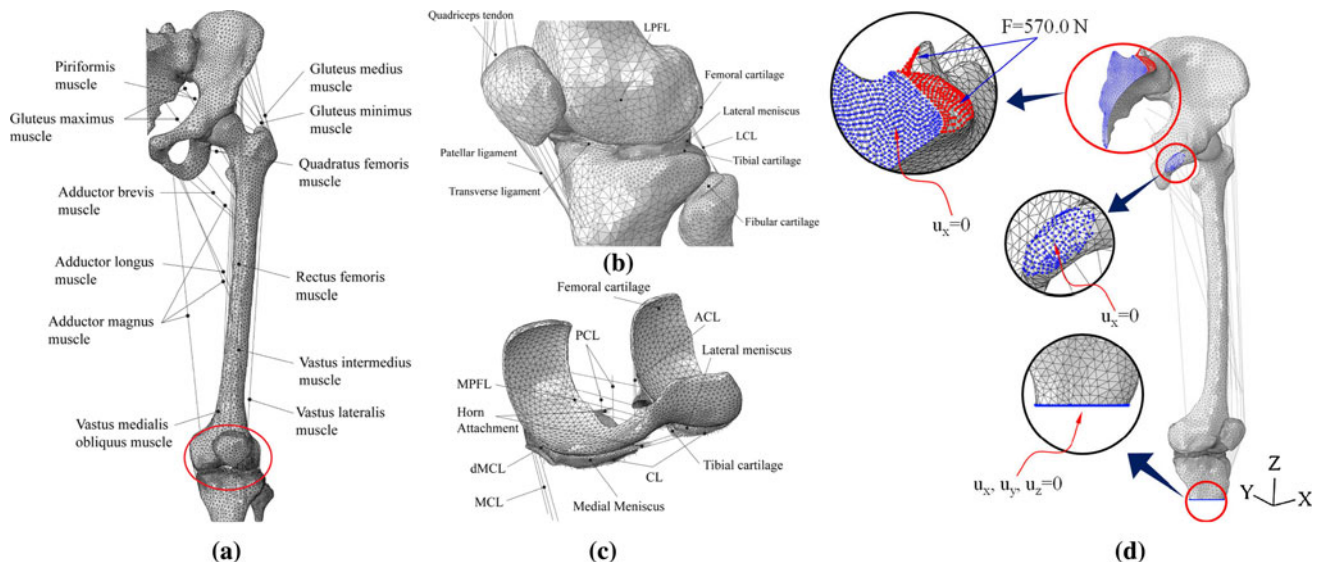


Fig. 1 Finite element model of the lower limb: **a** frontal view, **b** enlarged view of tibiofemoral joint part, **c** contact structure between cartilage and meniscus, and **d** boundary conditions for the computation

Table 1 Material properties of each tissue

| Tissue | Elastic modulus (MPa) | Poisson’s ratio | Reference |
|---|-----------------------|-------------------------|-----------|
| Bony structures (Sacrum, coxal bone, femur, tibia, fibula, patella) | Rigid | | |
| Femoral/tibial articular cartilage | 12 | 0.45 | [26] |
| Articular cartilage of the sacrum and acetabulum | 5 | 0.46 | [17] |
| Patellar cartilage | 7 | 0.47 | [4] |
| Lateral/medial meniscus | 59 | 0.49 | [16] |
| | Elastic modulus (MPa) | PCSA (mm ²) | Reference |
| Quadriceps tendon | 303.9 | 64.60 | [27] |
| Patellar ligament | 459.3 | 36.80 | [27] |
| Coronal ligament | 416.0 | 2.05 | [6] |
| Medial patellofemoral ligament | 19.1 | 42.70 | [2] |
| Lateral patellofemoral ligament | 17.0 | 28.50 | [2] |
| | Stiffness (N/mm) | | Reference |
| Transverse ligament | 900 | | [10] |
| Horn attachments | 200 | | [30] |

In general, the medial meniscus is attached more firmly to the tibial surface, and is injured more frequently than the lateral meniscus [1]. Therefore, medial meniscetomized models were considered. To examine the effects of meniscetomy, FE models of the intact meniscus and the partial, sub-total, and total medial menisci were developed after discussions with orthopedists. These models were used in our simulations as shown in Fig. 2.

The major ligaments in knee joints such as the anterior cruciate ligament (ACL), posterior cruciate ligament (PCL), medial collateral ligament (MCL), lateral collateral

ligament (LCL), and deep medial collateral ligament (dMCL) were modeled as one-dimensional (1D) nonlinear spring elements. The nonlinear characteristics of the elements are described as follows:

$$f = \begin{cases} 0.25k\varepsilon^2/\varepsilon_1 & 0 \leq \varepsilon \leq 2\varepsilon_1 \\ k(\varepsilon - \varepsilon_1) & \varepsilon > 2\varepsilon_1 \\ 0 & \varepsilon < 0 \end{cases} \quad (1)$$

where f is the force, k is the stiffness, ε is the strain, ε_1 is the nonlinear strain parameter, and the related constants are reported by Blankevoort et al. [7]. Each ligament was

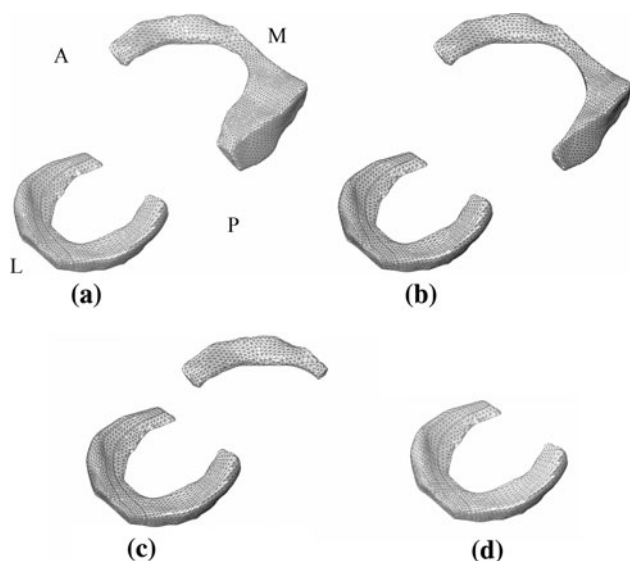


Fig. 2 Finite element meniscectomized models: **a** intact meniscus and **b–d** menisci under partial, sub-total, and total meniscectomy, respectively

attached at the anatomically appropriate site in the FE model, based on the MR images. The transverse ligament and the anterior/posterior meniscal horn attachment were modeled using 1D linear spring elements. The coronary ligament, the patellar ligament, the quadriceps tendon, the medial patellofemoral ligament (MPFL), and the lateral patellofemoral ligament (LPFL) were modeled using truss elements. The coronary ligament, patellar ligament, patellofemoral ligaments, and quadriceps tendon were considered to have a physical cross-sectional area (PCSA), and were assumed to be homogeneous, isotropic, and linear elastic materials as described in Table 1.

The quadriceps femoris muscles and the hip joint muscles were also modeled as 1D linear spring elements. The stiffness values for these muscles, assuming a single-leg stance, were determined as follows: muscle fiber-lengthening due to passive muscle stiffness equals the muscle fiber-shortening due to the active muscle contraction, as given by Phillips et al. [21].

2.4 Loads and boundary conditions

We included both the tibiofemoral joints and the sacroiliac joints for a realistic knee joint characterization, and applied an anatomically suitable boundary condition. This enabled the body weight to be applied at realistic locations, and helped generate an external adduction moment. Using the assumption of the single-leg stance under full extension, a vertical load of 570 N, corresponding to five-sixths of the body weight (70 kg), was applied on the sacrum through the center of the L5S1 disc and the facet of the sacral horn

[14]. The x-direction displacements of the nodes on the symmetric surfaces of the sacrum and coxal bones were fixed. In addition, the nodes on the distal surfaces of the tibia and fibula were fixed to prevent translation and rotation, as shown in Fig. 1c. The contact surfaces were defined between menisci and femoral articular cartilage, between menisci and tibial articular cartilage, and between acetabular cartilage and the femoral head. For all the contact surfaces, a frictionless contact condition was assumed by considering smooth joint movement due to synovial fluid. Then, a FEA was performed using the commercial software ABAQUS (v6.8.1, Dassult Systemes, France).

3 Results

Before performing the complete simulation, mesh convergence tests were performed using two different models with 238,101 elements and 440,963 elements of the intact knee joint model. The test results showed that in the cartilage-to-meniscus contact area, there were 1% difference between the model using 440,963 elements and the proposed model (338,588 elements), and 6.5% difference between the model using 238,101 elements and the proposed model. There were also in the peak contact pressures, 5% difference between the model using 440,963 elements and the proposed model, and 7% difference between the model using 238,101 elements and the proposed model. This means that the total number of elements in the proposed model is sufficient to solve this problem exactly. Thus, the suitability of the number of elements of the proposed model was confirmed.

First, the results obtained from the intact knee joint model were compared with previously reported experimental and computational results, as given in Table 2. The following terms are introduced: contact pressure in the medial meniscus (CPMM); contact pressure in the lateral meniscus (CPLM); contact area in the medial compartment (CAM); and contact area in the lateral compartment (CAL). Almost all the results in Table 2 show that the contact pressure in the medial meniscus was greater than that in the lateral meniscus, and the contact area in the medial compartment was larger than that of the lateral compartment [9, 13, 19, 20]. Furthermore, all the results show similar trends in the magnitudes of the contact pressure and the contact area, depending on the applied loading (although there are differences in the specimen structures and boundary conditions). We note that the model used in this study can yield reasonable analytic results because it includes the effects of the external adduction moment and the muscle forces of the hip joints on the knee joints.

Table 2 Comparison of the obtained results with published results for the intact knee joint

| | Method | Load | CPMM | CPLM | CAM | CAL | Reference |
|--------------------------|----------------|-------|------|------|--------------|---------------|-----------|
| Our model | FEA | 570 | 1.24 | 1.06 | 450.48 | 341.55 | |
| Fukubayashi and Kurosawa | Experiment | 500 | – | ~4 | 530 ± 150 | 420 ± 60 | [9] |
| Peña et al. | FEA | 1,150 | 2.90 | 1.45 | – | – | [19] |
| Ihn et al. | Experiment | 1,176 | – | – | 610 | 450 | [13] |
| Pèriè and Hobatho | FEA/Experiment | 500 | 1.57 | – | 354/283 ± 72 | 135/111 ± 150 | [20] |

CPMM contact pressure in the medial meniscus; CPLM contact pressure in the lateral meniscus; CAM contact area in the medial compartment; CAL contact area in the lateral compartment

Figure 3a–d shows the contact pressure distributions and contact areas in the menisci. Following various medial meniscectomies, the region of concentrated contact pressure and contact area decreased in the medial meniscus. However, in the lateral meniscus, slight changes were found in the contact pressure and the contact area. Figure 4 shows the contact pressure distribution and the contact area in the femoral and tibial articular cartilages, respectively. The concentrated contact pressures occurred on the cartilage-to-cartilage contact area of both the medial and lateral parts, and their regions were broadened on both the femoral and tibial cartilages, depending on the type of medial meniscectomy. The cartilage-to-meniscus contact areas on the femoral and tibial cartilages of the medial parts decreased depending on the type of meniscectomy. However, contact areas of the lateral parts were not significantly changed.

Figure 5a and b shows the cartilage-to-meniscus and cartilage-to-cartilage contact area changes obtained from Figs. 3 and 4. With greater removal of the meniscus, the cartilage-to-meniscus contact area in the medial compartment rapidly decreased from 253.41 to 0 mm². However, the cartilage-to-meniscus contact area in the lateral compartment increased by 16.78%, from 155.2 to 181.25 mm² (see Fig. 5a). The cartilage-to-cartilage contact area in the medial compartment gradually increased by 3.94%, from 197.08 to 204.84 mm², and the cartilage-to-cartilage contact area in the lateral compartment rapidly increased by 8.32%, from 186.36 to 201.86 mm², depending on the amount of medial meniscus that was removed (see Fig. 5b).

The peak contact pressure values obtained from Figs. 3 and 4 are plotted in Fig. 6a and b. In the medial menisci, the peak contact pressure rapidly increased by 70.82%,

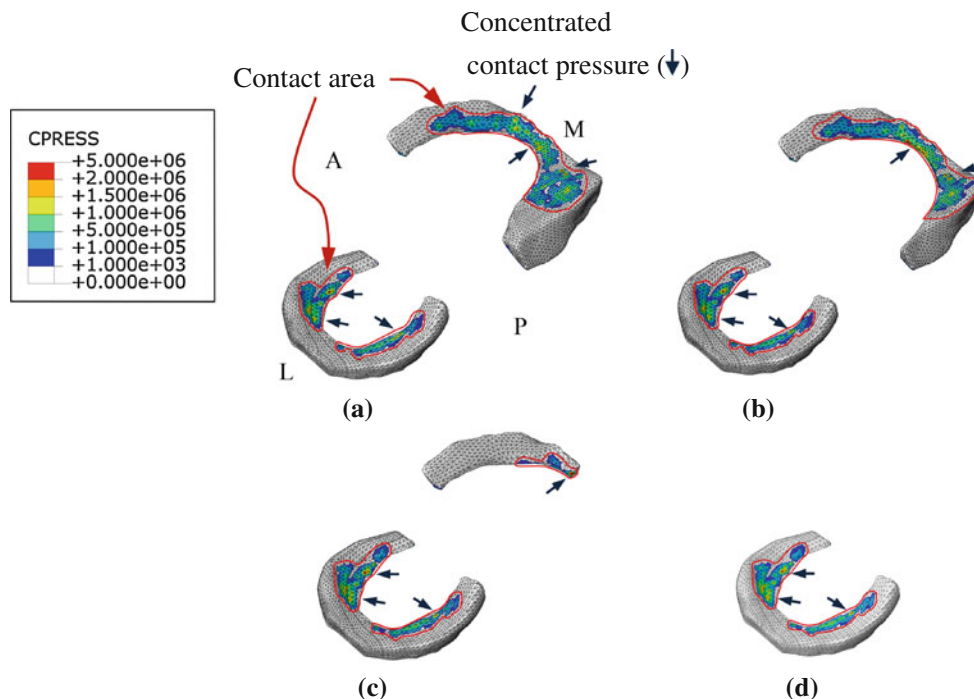
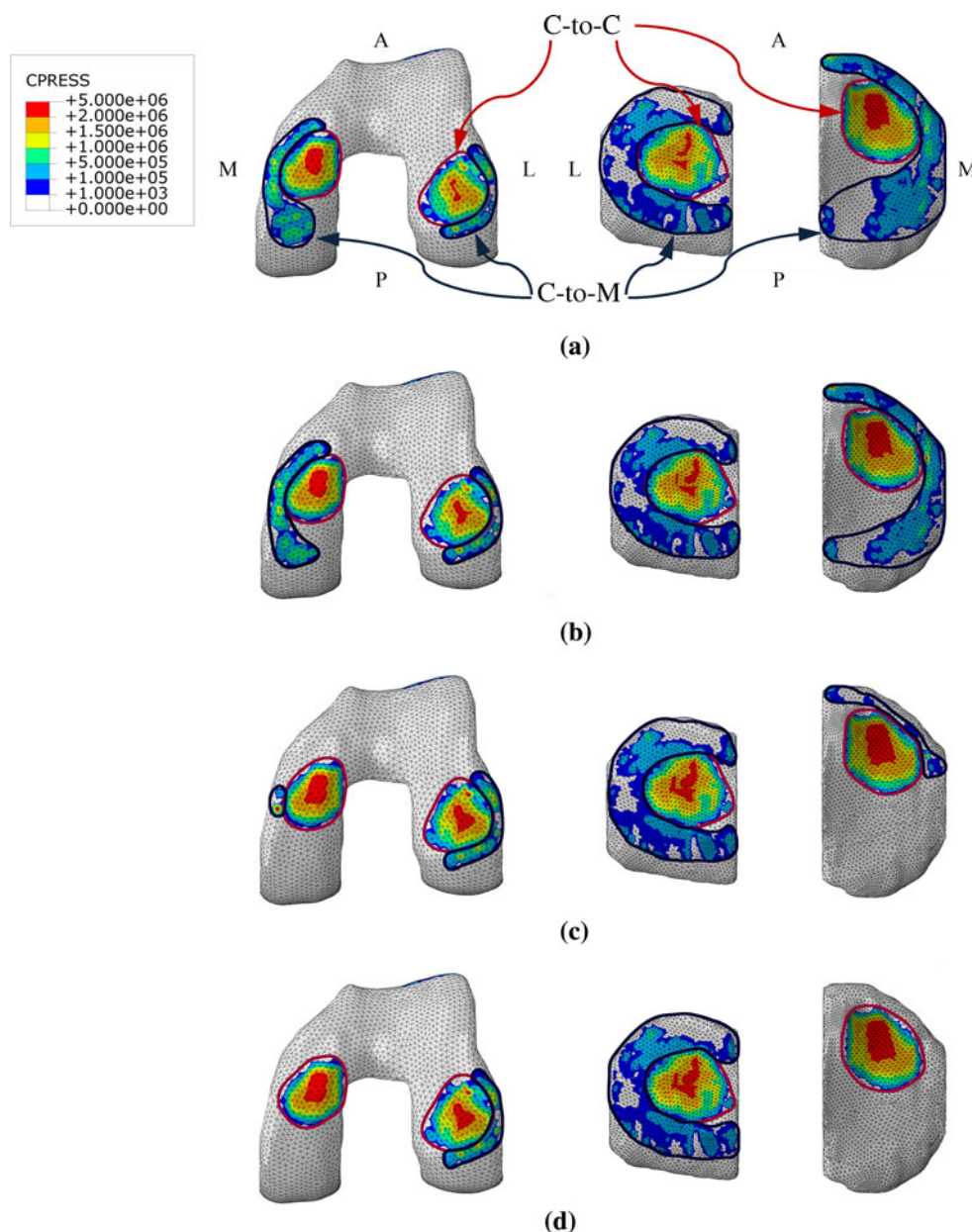


Fig. 3 Contact pressure distributions in: **a** intact meniscus and **b–d** menisci under partial, sub-total, and total meniscectomy, respectively

Fig. 4 Contact pressure distributions in the femoral and tibial articular cartilages following (a) no meniscectomy and b–d partial, sub-total, and total medial meniscectomy, respectively



from 2.57 to 4.39 MPa, depending on the amount of meniscus that was removed. In the lateral menisci, the peak contact pressure gradually increased by 11.45%, from 2.27 to 2.53 MPa, after a partial meniscectomy, and by 23.79%, from 2.27 to 2.81 MPa, after a subtotal meniscectomy. The peak contact pressure increased rapidly by 94.27%, from 2.27 to 4.41 MPa, after a total meniscectomy (see Fig. 6a). In the medial femoral articular cartilage after total meniscectomy, an increase in the peak contact pressure of 29.31%, from 2.32 to 3.00 MPa, was observed. In the lateral part, an increase in the peak contact pressure of 27.06%, from 2.18 to 2.77 MPa, was observed. In the medial tibial articular cartilage, a 26.34% increase in the

peak contact pressure, from 2.62 to 3.31 MPa, was observed; in the lateral part, a 18.70% increase in the peak contact pressure, from 2.46 to 3.06 MPa, was observed (see Fig. 6b).

4 Discussion

We analyzed contact pressures and contact areas in knee joints after various types of medial meniscectomy procedures. Our results show that following the procedures, the cartilage-to-cartilage contact area in both the medial and lateral compartments increased significantly compared to

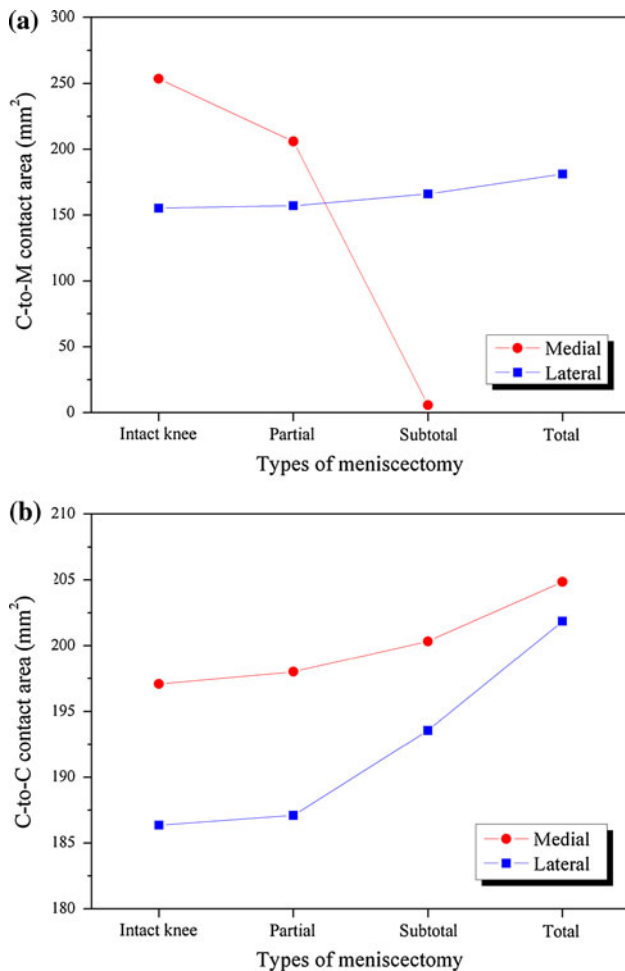


Fig. 5 **a** Cartilage-to-cartilage contact area and **b** cartilage-to-meniscus contact area, depending on the type of meniscectomy

the cartilage-to-meniscus contact area. The peak contact pressure in the meniscus increased significantly, but showed a slow increase in articular cartilage depending on the type of meniscectomy. Therefore, we consider that the cartilage-to-cartilage contact area and the peak contact pressure in the meniscus may be significant parameters for evaluating degenerative osteoarthritis based on the effects of contact area and contact stress on degenerative osteoarthritis, as reported by Fukubayashi and Kurosawa [9] and Segal et al. [26].

In particular, the cartilage-to-cartilage contact area and the peak contact pressure in the lateral menisci increased significantly after total meniscectomy. This is due to a change in load transmission in the knee joints that stems from the loss of mechanical function of the medial meniscus. However, after partial meniscectomy, no serious increase was found in the contact areas and in the peak contact pressures in both the medial and lateral compartments. Therefore, a high possibility of degenerative

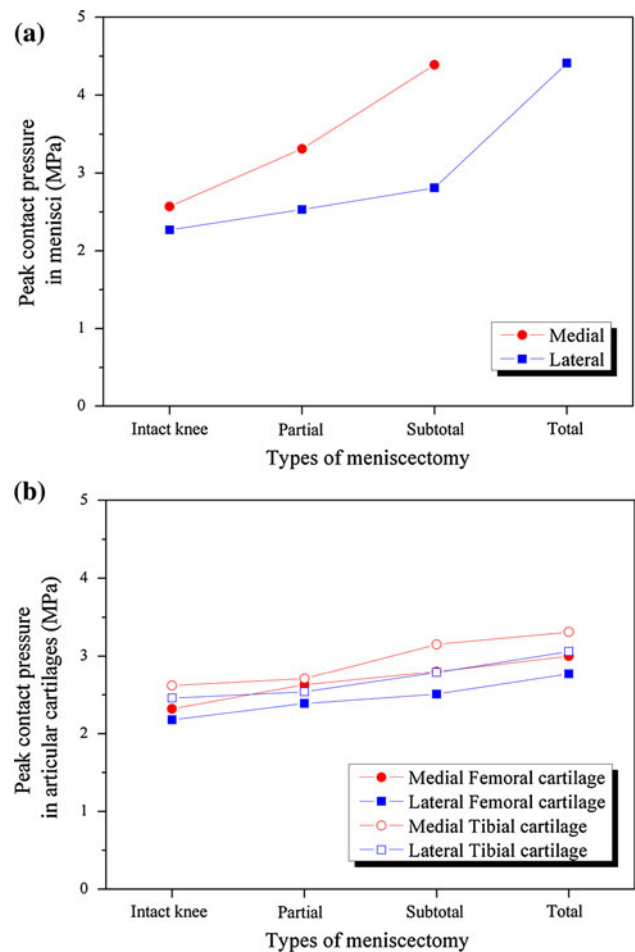


Fig. 6 Peak contact pressures in **a** menisci and **b** articular cartilages, depending on the type of meniscectomy

osteoarthritis after total meniscectomy is anticipated, and partial meniscectomy can be regarded as a better treatment than subtotal/total meniscectomy [11, 18].

One interesting finding is that the contact areas and the peak contact pressures in the lateral compartment increased after medial meniscectomy. This phenomenon occurs due to the change in load transfer caused by the removal of the medial meniscus; thus, medial meniscectomy has the potential to bring about degenerative osteoarthritis in the lateral compartment of a knee joint. In particular, the method of biomechanical analysis in this research can be extended to decide significant parameters and to analysis their effects on osteoarthritis of a hip joint [22], and also be used for designing and fabricating artificial cartilages to treat the degenerative osteoarthritis [24].

Acknowledgments This study was supported by the Nuclear R&D Program through the National Research Foundation of Korea funded by the Ministry of Education, Science, and Technology of the Korean government (No. 2009-0093620).

References

- Allen AA, Caldwell GL, Fu FH (1995) Anatomy and biomechanics of the meniscus. *Oper Tech Orthop* 5:2–9
- Atkinson P, Atkinson T, Huang C, Doane R (2000) A comparison of the mechanical and dimensional properties of the human medial and lateral patellofemoral ligaments. In: Proceedings of the 46th annual meeting of the Orthopaedic Research Society, Orlando, FL, USA
- Baratz ME, Fu FH, Mengato R (1986) Meniscal tears: the effect of meniscectomy and of repair on intraarticular contact areas and stress in the human knee. A preliminary report. *Am J Sports Med* 14:270–275
- Beaupré GS, Carter DR (1992) Finite element analysis in biomechanics. In: Biewener AA (ed) *Biomechanics: structures and systems a practical approach*. Oxford University Press, Oxford, pp 149–174
- Bendjaballah MZ, Shirazi-Adl A, Zukor DJ (1995) Biomechanics of the human knee joint in compression: reconstruction, mesh generation and finite element analysis. *Knee* 2:69–79
- Bendjaballah MZ, Shirazi-Adl A, Zukor DJ (1997) Finite element analysis of human knee joint in varus-valgus. *Clin Biomech (Bristol, Avon)* 12:139–148
- Blankevoort L, Kuiper JH, Huijskes R, Grootenboer HJ (1991) Articular contact in a three-dimensional model of the knee. *J Biomech* 24:1019–1031
- Burke DL, Ahmed AH, Miller J (1978) A biomechanical study of partial and total medial meniscectomy of the knee. *Trans Orthop Res Soc* 3:91
- Fukubayashi T, Kurosawa H (1980) The contact area and pressure distribution pattern of the knee: a study of normal and osteoarthrotic knee joints. *Acta Orthop Scand* 51:871–879
- Haut Donahue TL, Hull ML, Rashid MM, Jacobs CR (2002) A finite element model of the human knee joint for the study of tibio-femoral contact. *J Biomech Eng* 124:273–280
- Hede A, Larsen E, Sandberg H (1992) The long term outcome of open total and partial meniscectomy related to the quantity and site of the meniscus removed. *Int Orthop* 16:122–125
- Hoser C, Fink C, Brown C, Reichkandler M, Hackl W, Bartlett J (2001) Long-term results of arthroscopic partial lateral meniscectomy in knees without associated damage. *J Bone Joint Surg (Br)* 83:513–516
- Ihn JC, Kim SJ, Park IH (1993) In vitro study of contact area and pressure distribution in the human knee after partial and total meniscectomy. *Int Orthop* 17:214–218
- Jeon I, Bae JY, Park JH, Yoon TR, Todo M, Mawatari M, Hotokebuchi T (2011) Biomechanical effect of the collar of femoral stem on total hip arthroplasty. *Comput Methods Biomech Biomed Eng* 14:103–112
- Jones RE, Smith EC, Reisch JS (1978) Effects of medial meniscectomy in patients older than forty years. *J Bone and Joint Surg (Am)* 60A:783–786
- LeRoux MA, Setton LA (2002) Experimental biphasic fem determinations of the material properties and hydraulic permeability of the meniscus in tension. *J Biomech Eng* 124:315–321
- Li G, Lopez O, Rubash H (2001) Variability of a three-dimensional finite element model constructed using magnetic resonance images of a knee for joint contact stress analysis. *J Biomech Eng* 123:341–346
- McGinity JB, Geuss LF, Marvin RA (1997) Partial or total meniscectomy: a comparative analysis. *J Bone and Joint Surg (Am)* 59:763–766
- Peña E, Calvo B, Martinez MA, Palanca D, Doblaré M (2005) Finite element analysis of the effect of meniscal tears and meniscectomies on human knee biomechanics. *Clin Biomech (Bristol, Avon)* 20:498–507
- Pèriè D, Hobatho MC (1998) In vivo determination of contact areas and pressure of the femorotibial joint using non-linear finite element analysis. *Clin Biomech (Bristol, Avon)* 13:394–402
- Phillips AT, Pankaj P, Howie CR, Usmani AS, Simpson AH (2007) Finite element modelling of the pelvis: inclusion of muscular and ligamentous boundary conditions. *Med Eng Phys* 29:739–748
- Pustoc'h A, Cheze L (2009) Normal and osteoarthritic hip joint mechanical behaviour: a comparison study. *Med Biol Eng Comput* 47:375–383
- Rangger C, Klestil T, Gloetzer W, Kemmler G, Benedetto KP (1995) Osteoarthritis after arthroscopic partial meniscectomy. *Am J Sports Med* 23:240–244
- Sato M, Ishihara M, Furukawa K, Kaneshiro N, Nagai T, Mitani G, Kutsuna T, Ohta N, Kokubo M, Kikuchi T, Sakai H, Ushida T, Kikuchi M, Mochida J (2008) Recent technological advancements related to articular cartilage regeneration. *Med Biol Eng Comput* 46:735–743
- Seedhom BB, Hargreaves DJ (1979) Transmission of the load in the knee joint with special reference to the role of the menisci. *Eng Med* 8:207–228
- Segal NA, Anderson DD, Iyer KS, Baker J, Torner JC, Lynch JA, Felson DT, Lewis CE, Brown TD (2009) Baseline articular contact stress levels predict incident symptomatic knee osteoarthritis development in the MOST cohort. *J Orthop Res* 27:1562–1568
- Stäubli HU, Schatzmann L, Brunner P, Rincón L, Nolte LP (1999) Mechanical tensile properties of the quadriceps tendon and patellar ligament in young adults. *Am J Sports Med* 27:27–34
- Wilson W, van Rietbergen B, van Donkelaar CC, Huijskes R (2003) Pathways of load-induced cartilage damage causing cartilage degeneration in the knee after meniscectomy. *J Biomech* 36:845–851
- Yang N, Nayeb-Hashemi H, Canavan PK (2009) The combined effect of frontal plane tibiofemoral knee angle and meniscectomy on the cartilage contact stresses and strains. *Ann Biomed Eng* 37:2360–2372
- Zielinska B, Donahue TL (2006) 3D finite element model of meniscectomy: changes in joint contact behavior. *J Biomech Eng* 128:115–123